RSC Pharmaceutics

ROYAL SOCIETY OF CHEMISTRY

PAPER

View Article Online
View Journal | View Issue

Check for updates

Cite this: *RSC Pharm.*, 2025, **2**, 570

Polysaccharide-capped silver nanoparticles impregnated cream for the efficient management of wound healing†

H. P. Syama,[a] B. S. Unnikrishnan,[a,b] J. Sreekutty,[a] M. G. Archana,[a] G. U. Preethi,[a,b] P. L. Reshma[a] and T. T. Sreelekha *[a]

Received 20th September 2024,
Accepted 23rd February 2025

DOI: 10.1039/d4pm00274a

rsc.li/RSCPharma

Developing wound-dressing materials that meet all the required qualities for curing burns and injuries caused by various diseases is a challenging task. However, the biocompatibility, biodegradability, and non-toxicity of natural polysaccharides make them an excellent base material for creating flexible and widely accepted formulations. To test this, we created a cream formulation that utilised galactomannan's non-toxic and immuno-stimulatory properties and added silver nanoparticles to create SNP@PSP. Preclinical studies were conducted *in vitro* and *in vivo* experiments in rat models to test the wound-healing capabilities of the formulation. The cream's ability to heal wounds was demonstrated through immunohistochemistry, collagen staining, and histopathology. Our work provides a formulation that utilises silver nanoparticles to create polysaccharide cream with improved biocompatibility and antibacterial properties. The rat wound-healing experiments showed that the cream was effective for clinical use, with the addition of nanosilver significantly boosting its antibacterial properties.

1. Introduction

The global wound-care market was valued at USD 20.6 billion in 2021, and from 2022 to 2030, it is projected to grow at a compound annual growth rate (CAGR) of 4.1%.[1] Skin injuries significantly impact the world's healthcare systems and place heavy strains on the economy and society. The healing process is accelerated with less scarring when wounds are adequately cared for, minimising infection and other issues.[2] Various methods are employed to accelerate the healing of wounds. Alternative or complementary treatments utilising natural chemicals are in considerable demand. Additionally, topical medicine administration is favoured because it has no adverse effects on other organs.[3]

Due to their excellent biocompatibility compared to other substances, natural polysaccharides are widely used to diagnose many diseases. In addition, natural polysaccharides are poor immunogens, *i.e.*, they do not trigger an immunological reaction.[4–8] This add-on benefit guarantees that immune cells won't eliminate the substance from the body. These substances are excellent alternatives for creating products that can be used for wound healing.[9] They can also promote cell proliferation, tissue repair of normal cells, and antibacterial activity.

When used as a wound-healing agent, natural polysaccharides demonstrate several means to accomplish early recovery, including improved angiogenesis of the injured site's blood vessels, cell signalling, and development.[10–12] Specific polysaccharides inhibit the growth of microorganisms, which cause prolonged injury and lengthy healing periods. The field of nanomedicine has been revolutionised by the application of nanotechnology concepts in diagnosing and treating various diseases. Silver nanoparticles are known for their exceptional antibacterial properties and have found widespread use in biomedical applications.[16–18] These tiny particles have been found to induce the production of reactive oxygen species (ROS), leading to oxidative stress and cellular damage, including irregularities in the cell membrane, such as pits and accumulation.[15] They have been proven to be effective against multi-drug-resistant organisms as well as Gram-positive and Gram-negative bacteria.[19] Polysaccharide (PSP001) isolated from *Punica granatum*, a member of the Lythraceae family, has been reported to have various therapeutic benefits, including anti-cancer, antioxidant, and antibacterial action.[8,13–15,21] Several metal nanoconjugates have been synthesised using PSP001 and studied for their antitumor and immunomodula-

[a]*Laboratory of Biopharmaceuticals and Nanomedicine, Division of Cancer Research, Regional Cancer Centre (RCC), Medical College P.O., Thiruvananthapuram-695011, Kerala, India. E-mail: ttsreelekha@gmail.com, sreelekhatt@rcctvm.gov.in; Fax: +04712522378; Tel: +04712522378*
[b]*Department of Pathology, Dalhousie University, Nova Scotia, Canada*
† Electronic supplementary information (ESI) available. See DOI: https://doi.org/10.1039/d4pm00274a

tory activities. Previously, our group synthesised SNP@PSP using silver nanoparticles conjugated with PSP001 and its *in vitro* and *in vivo* antitumor efficacy was demonstrated.[20,21] Furthermore, in the present study we aim to develop a cream-based formulation using SNP@PSP for wound-healing application.

2. Experimental section

2.1. Materials

Stearic acid, isopropyl myristate, glycerine, EDTA, and all other chemicals used in cream formulations were obtained from Merck Millipore, USA. The cell line employed for the investigation was HaCaT (NCCS, Pune), the human keratinocyte line. GE Healthcare Life Sciences, Hyclone, was the supplier of Dulbecco's Modified Eagle's Medium (DMEM). An antibiotic–antimycotic combination and foetal bovine serum (FBS) were acquired from Gibco Life Technologies Corporation in the United States. The source of silver nitrate was Sisco Research Laboratories, located in Mumbai. The supplier of MTT (3-(4,5-dimethylazol-2-yl)-2,5-diphenyl-2*H*-tetrazolium bromide) was Sigma-Aldrich, whereas Merck was the source of the other AR-grade chemicals. An Indian company, Tarsons, supplied the plastic goods needed for cell culturing.

2.2. Methods

2.2.1. Formulation of SNP@PSP cream

2.2.1.1. Isolation of PSP001. The powdered rind of *Punica granatum* was first treated with petroleum ether to eliminate fats. A hot extraction process was conducted, and the mixture was centrifuged. The supernatant obtained was precipitated with 70% ethanol, and the aqueous phase was separated using chloroform. This aqueous phase was then dialysed with a dialysis membrane and concentrated through lyophilisation.[8] The resulting product, PSP001, was later preserved for synthesising silver nanoparticles (SNP@PSP).

2.2.1.2. Synthesis of SNP@PSP. Silver nanoparticles were prepared by slowly adding PSP001 (10 mg mL^{-1}) to a 1 mM solution of $AgNO_3$. The mixture was stirred at 460 rpm with a magnetic stirrer (Tarsons) and maintained at 60 °C for 24 hours or until the solution turned dark yellow, signifying the formation of nanoparticles.[20,21] The solution was then purified by dialysis against triple-distilled water using a cellulose membrane (Spectra/Por, MWCO 12 000–14 000 Da). Following purification, it was lyophilised, and the final product was stored at 4 °C for later use.

2.2.1.3. Preparation of SNP@PSP cream. The cream base was prepared by heating the oil and water phase components separately to 80 °C with gentle stirring. The oil phase included emulsifiers, emollients, thickeners, and preservatives, while the water phase contained chelating agents and sunscreen. After reaching the desired temperature, the oil phase was slowly combined with the water phase and homogenised using a mechanical stirrer (REMI Lab stirrer, RQ-129-D) at 2500 rpm for 10 minutes. Glycerine (1%) was added to the homogenised mixture when it had cooled to 50 °C, and stirring was continued until it reached room temperature (Table 1). To formulate the SNP@PSP creams, silver nanoparticles were mixed into the water phase at different concentrations, resulting in three variations: 0.1% (SNP@PSP cream 2), 0.5% (SNP@PSP cream 3), and 1% (SNP@PSP cream 4). A control cream without SNP@PSP was also prepared. The creams were packaged in 5 g aluminium tubes and stored at 25 °C and 60% humidity for further testing. The silver content in each cream formulation was studied by using an ICP-OES method.

2.2.1.3.1.Organoleptic characteristics

ESI Table 1† indicates the tests that were conducted on all formulations to assess their physical characteristics, including homogeneity, phase separation, colour, and texture. Visual observation was used to determine these qualities. A tiny amount of the prepared cream was pressed between the thumb and index finger to assess the cream's homogeneity and texture. The texture and homogeneity of the formulations were evaluated based on their consistency and the existence of coarse particles. Evaluation was also done on the immediate skin feel, which included greasiness, stiffness, and grittiness. The data explain the tests conducted for the cream's stability study.

2.2.1.3.2.Spreadability

The spread diameter of one gram of the sample applied after a minute in between two horizontal glass plates (10 cm × 20 cm) was used to measure the spreadability of the formulations. 50 g was the usual weight applied to the upper plate. Every formulation underwent three tests.

2.2.1.3.3.Formulation pH values

Using a pH meter, the pH of each formulation was determined (Cole-Parmer Instruments, pH tester, USA) after one gram was mixed with 25 millilitres of deionised water. There were three separate measurements taken. Before each usage, the pH meter was calibrated using standard buffer solutions with pH values of 4, 7, and 10.

2.2.2. Evaluation of antimicrobial activity of SNP@PSP and SNP@PSP-incorporated cream. The antimicrobial effectiveness of SNP@PSP was examined using well diffusion and disc

Table 1 Formulation of SNP@PSP cream

Phase	Ingredients	Qty in % wt/wt
A	Emulsifiers – stearic acid	10.0
	Thickeners/emollients (isopropyl myristate)	0.5
	Preservatives (propyl paraben, methylparaben)	0.375
	Skin penetrating agent (mineral oil)	5.0
	Moisturisers (glycerine)	1.0
B	Sterile DM water	65.0
	Chelating agent (EDTA disodium salt)	0.050
C	Sterile DM water	5.00
	pH adjuster and surfactant (potassium hydroxide)	0.1–0.40
D	DM water	1–3
	SNP@PSP	0.1 to 1
F	Sterile DM water	qs to 100
	Total	100.000

diffusion techniques. On Muller Hinton agar (MHA) plates, 6 mm diameter wells were drilled using a sterile cork borer for good diffusion. This investigation used *Staphylococcus aureus*, *Escherichia coli*, *Klebsiella pneumonia*, *Salmonella typhi*, *Candida albicans* and *Candida krusei* as test pathogens. Different SNP@PSP concentrations (each of volume 0.1 mL) were added to each well. The plates were incubated for 24 hours at 37 °C, keeping positive and negative controls. In the disc approach, SNP@PSP was impregnated into paper discs that were 6 mm in diameter at varying concentrations. As negative control, a paper disc devoid of SNP@PSP was placed in the middle of the plates and incubated. Following incubation, the diameter of the zone of inhibition for the well diffusion method and the disc diffusion method was measured to assess the susceptibility pattern of the test.

Each cream formulation was accurately weighed to 1 g. The cream formulation was then emulsified in a few drops of Tween 20, and further dilutions were prepared using 10% DMSO for the antimicrobial assay.

In vitro, the antibacterial activity of cream formulations was checked against *S. aureus*, *E. coli*, *K. pneumonia*, *S. typhi*, *C. albicans* and *C. krusei* by well diffusion assay and disc methods. For 18 hours, the infected MHA plate was incubated at 37 °C. A ruler was used to measure the observed sizes of the inhibitory zones to the closest millimetre. The quality, safety and reliability of SNP@PSP-incorporated cream was evaluated according to the guidelines laid down by the Bureau of Indian Standards (BIS) as described in the data of ESI S2–S5.†

2.2.3. Rheological measurements. These analyses are essential to evaluate factors such as stability, spreadability, drug release, and skin permeation. A controlled shear rheometer (MCR 302, Anton Paar, Germany) equipped with parallel plates (18 mm diameter) was used for rheological testing. The gap size was set to 1 mm, with a trimming gap of 550 μm to remove excess material. Each cream sample weighing 100 mg was carefully placed on the plate for analysis. All tests were conducted at a controlled temperature of 25 °C to ensure consistency.

The testing protocol comprised several steps to evaluate the cream's rheological behaviour.

(i) Shear rate test: this involved applying a shear rate ranging from 0.1 to 100 s^{-1} to assess the flow behaviour of the cream and its transition between liquid-like and solid-like states. (ii) Thixotropic test: the sample was subjected to shear rates from 0.1 to 100 s^{-1} to study the recovery of the cream's structure after the cessation of applied stress. (iii) frequency sweep test: the angular frequency (ω) was varied from 0.01 to 100 rad s^{-1} to understand the network's frequency-dependent viscoelastic behaviour. This standardized protocol provided a comprehensive understanding of the viscoelastic and flow properties of the cream formulations.[22–25]

2.2.4. *In vitro* cytotoxicity assay in human keratinocyte cell lines (HaCaT). To check whether the nanoparticles are toxic to normal cell lines, the growth inhibitory capacity of the nanoparticles was evaluated in the HaCaT cell line by using the MTT (3-(4, 5-dimethylthiazol-2yl)-2, 5 diphenyltetrazolium) assay.[5] A MicroTek Power Wave XS microplate spectrophotometer measured the absorbance at 570 nm. The following formulas were used to determine the rates of proliferation and inhibition of the cells:

$$\text{Proliferation rate (PR)}\% = \left[\frac{\text{Abs}_{\text{sample}} - \text{Abs}_{\text{blank}}}{\text{Abs}_{\text{control}} - \text{Abs}_{\text{blank}}}\right] \times 100$$

$$\text{Inhibitory rate (IR)}\% = 100 - \text{PR}$$

MTT assays were performed on HaCaT cells with various concentrations of nanoparticles for 72–96 h.

2.2.5. *In vitro* wound-healing activity. HaCaT cells at a concentration of 1×10^6 cells per mL were cultivated in DMEM on Ibidi 2-well silicone culture inserts from Germany, which featured a well-defined cell-free gap for *in vitro* wound-healing studies.[26] After 24 hours, the culture insert was removed to initiate the gap formation. The test materials were introduced into the cells, which were maintained at 37 °C in a 5% CO_2 incubator. The cells were observed using a phase-contrast microscope (Olympus 1X 51, Singapore) with a 10× objective at different intervals (0, 12 h, 24 h, up to 120 h) until the monolayer was completely closed. The change in wound closure area was measured using ImageJ software (wound healing size tool). Using this software, the wound area was calculated using the area tool and MRI wound healing tool.

$$\text{Wound closure}\% = 100 - \text{wound area}\%$$

2.2.6. *In vivo* wound healing using SNP@PSP cream

2.2.6.1. Experimental animals. The trials on wound healing employed 150–200 g (6–8 weeks old) Wistar rats (albino outbred strain). A total of 16 healthy rats were used and divided equally ($n = 4$) into four groups as follows: group I, control considered as untreated with skin covered with gauze; group II, positive control Silverex-treated group; group III, base cream-treated group; group IV: SNP@PSP cream-treated group. Group IV SNP@PSP cream-treated rats were selected for the *in vivo* studies. Before the commencement of the tests, the animals were housed in a laboratory setting under 26 °C ± 2 °C, 60–70% relative humidity, and 12 hour light and dark cycle conditions for seven days. The Institutional Animal Ethical Committee approved all the experimental methods and procedures utilised in this work, all produced by CPCSEA criteria. The animals were fed pellets and given unlimited access to water. The study was performed according to ARRIVE guidelines.

2.2.6.2. Punch wound model. Briefly, intraperitoneal (i.p.) injections of xylazine (10 mg kg^{-1}) and ketamine (80 mg kg^{-1}) were used to put the animals to sleep. After the anaesthesia, 70% ethanol was used to clean the area, and a commercial hair remover was used to remove the dorsal hair. Full-thickness excisions of 8 mm in diameter were made using a biopsy punch. After excisions, SNP@PSP cream was applied to the wound immediately on the corresponding animals. Special care was taken to maintain aseptic conditions throughout all the experiments. SNP@PSP cream, base cream and Silverex were applied continuously for 21 days.

2.2.6.3. Determination of wound healing rate. Using vernier callipers (Aerospace 300 mm), the wound size was assessed on

0, 3, 7, and 14 days to evaluate the therapeutic effectiveness of the proposed nanoformulation on the injured site. The animals were observed daily, and no adverse effects were observed following topical treatments. As a result, the following equation was used to calculate the percentage (%) contraction of the wound using this model: percentage wound contraction = (wound area of day '*N*'/wound area of day 0) × 100.

2.2.6.4. Microbiological examination of the wound area. On the 3rd, 7th, 14th and 21st days, swabbing was done on nutrient agar plates; the sample was collected from the wound area from each group to determine the number of colony-forming units (CFU) present in the wound. CFU was calculated using the pour plate method. Serial dilutions were done up to 10^{-5}, and plating was done from 10^{-1} to 10^{-2}. Plates were incubated for 24 h, and the total viable count (TVC) was calculated.

2.2.6.5. H&E and immunohistochemistry. After dissecting, the skin wound samples were preserved in 4% paraformaldehyde. Paraffin-embedded samples were placed in gradient alcohol. Tissue sections of five micrometres were cut and placed on glass slides. The sections underwent the following steps for H&E staining: xylene dewaxing, gradient alcohol rehydration, distilled H_2O washing, Harris haematoxylin solution staining, 0.3% acid alcohol differentiation, and eosin staining. The sections were cleaned in xylene and mounted using a xylene-based mounting media following another dehydration stage in gradient alcohol. The tissues were treated with an MTS staining solution in preparation for Masson's trichrome staining test. The sections were dewaxed in xylene and then pre-treated with antigen retrieval solution (pH = 9.0 EDTA solution) for immunohistochemical experiments. The sections were then stained with the appropriate antibodies (Cox 2; VEGF) (Abcam ab208670, 1 : 100) according to the manufacturer's introduction, and then the images were scanned using 3DHISTECH CaseViewer 2.4.[27]

2.2.7. Statistical analysis. The results are presented as the mean ± standard deviation (SD) from three independent replicates. Statistical analysis was performed using GraphPad Prism version 8.0.1, applying one-way analysis of variance (ANOVA) (GraphPad, La Jolla, CA, USA). Results are expressed as mean ± SD, with significance levels indicated as follows: * ($p < 0.01$), ** ($p < 0.001$), and *** ($p < 0.0001$).

3. Results & discussion

3.1. Formulation of cream

SNP@PSP with immunostimulatory ability exhibits appreciable therapeutic value with its tumour-selective properties.[28] The morphology of the synthesized SNP@PSP was analysed under transmission electron microscopy and particles were found to be 25 ± 5 nm (ESI Fig. 1†). SNP@PSP wipes out signs of acute and subacute toxicity in *in vivo* rodent models associated with SNPs. Including SNP@PSP in a cream formulation is expected to simulate an appropriate anti-bacterial environment for wound healing. In the study, base cream 1 and SNP@PSP cream formulations 2–4 were prepared using different concentrations of SNP@PSP. The creams were of good consistency (Fig. 1A). Homogeneity and texture were adequate for topical application. Each cream was found to be free from grittiness and was non-sticky. Organoleptic characteristics are shown in ESI Table 2.† The ICP-OES analysis revealed that the silver content in SNP@PSP creams 2, 3, and 4 was 0.062 mg, 0.31 mg, and 0.62 mg per gram of cream, respectively. These values were significantly lower than the permissible limits. Spreadability is the capacity of a cream to be distributed throughout the skin. The effectiveness of topical therapy and the application of a standard dose of a medicinal cream formulation to the skin are significantly influenced by spreadability. The topical cream is still beneficial if its spreadability is reduced because it is simple to apply to the skin. One minute after application, the area of the tested cream is measured by a scale to determine the diameter of the circle formed by the cream. The average diameter of spreadability of each formulation is shown in Fig. 1C. The diameter for base cream 1 was 5.2 cm, that for SNP@PSP 2 was 3.5 cm, that for SNP@PSP cream 3 was 2.5 cm, and that for SNP@PSP cream 4 was 2.5 cm. This showed that our formulated cream was suitable for skin care applications. The pH of all formulated cream samples was examined. The results showed that all creams are compatible with skin pH (Fig. 1B). The addition of SNP@PSP can reduce the alkaline nature of the base cream.

In a stability test, product samples were placed in various environments for predetermined amounts of time to mimic potential outcomes for the product's life cycle. Samples were assessed for multiple physical, chemical, and performance traits at predetermined intervals to see whether and how they had changed (ESI Table 2†). No change was observed in the cream formulation's organoleptic and physicochemical properties, demonstrating stability.

One of the most crucial tests that needs to be carried out is the weight loss evaluation, which measures the amount of water that evaporates through the container wall. This test was conducted on samples stored at room temperature, 45 °C and 4 °C for two months (ESI Table 3†). At 45 °C, SNP@PSP cream showed a weight loss of about 2.92%; typically, cream formulations are not stored at this elevated temperature, which is a point to note here. No weight loss was observed at 4 °C and at room temperature (ESI Table 4†). The cream formulation was taken for analysis as per the BIS. The results obtained are shown in ESI Table 5.† As per these results, our formulated SNP@PSP cream complies with all parameters and BIS specifications.

Since the antimicrobial activity was most pronounced in the SNP@PSP cream (cream 4), both this cream and the base cream were subjected to rheological analysis to understand their behaviour during processing, packaging, and storage. Rheological parameters like flow sweep and yield stress are critical indicators of a cream's viscosity and ease of spreadability, which influence both application and the delivery of active ingredients across the skin. In this study, rotational rheological tests were used to characterize these properties in all cream formulations. Results showed that all formulations exhibited

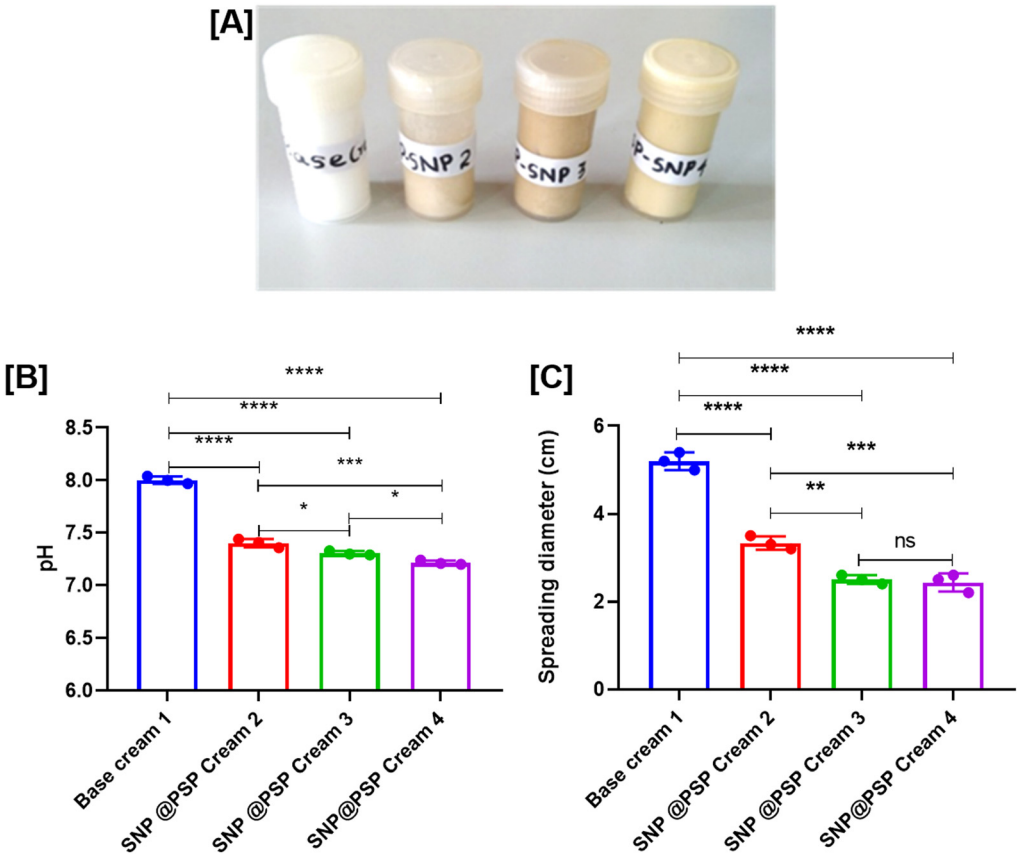

Fig. 1 (A) Base cream and SNP@PSP cream formulations; (B) pH values of formulated creams (n = 3); and (C) graphical representations of cream spreading diameter (n = 3).

viscoelastic behaviour and demonstrated similar performance in spreading when strain was applied. This suggests that the formulations maintain a balance between structural integrity and usability, making them suitable for topical application. The difference in viscosity between the two formulations could be due to variations in composition or the incorporation of SNP@PSP (presumably a nanoparticle system). The lower viscosity of the SNP@PSP cream could make it easier to spread (ESI Fig. 2†). Both creams show shear-thinning behaviour, where viscosity decreases as shear rate increases. This is typical for creams, gels, or suspensions. Lower viscosity may make the SNP@PSP cream more suitable for applications requiring smoother and easier application compared to the base cream (ESI Fig. 3†).

3.2. Antimicrobial activity of cream formulation

It is well known that several silver nanoparticles are found to exhibit antimicrobial activity in a broad spectrum of biomedical applications. However, polysaccharide-capped silver nanoparticles were found to be more effective in versatile biomedical applications due to their unique feature of immunomodulation.[29] The antimicrobial activity was checked against *S. aureus*, *E. coli*, *K. pneumonia*, *S. typhi*, *C. albicans* and *C. krusei*. SNP@PSP showed significant antimicrobial activity against *S. aureus*, *C. albicans* and *C. krusei* (Fig. 2 and ESI Tables 6, 7†). These organisms are predominant in skin infections, and hence, the results confirmed that SNP@PSP could be used as an effective agent against skin infections. The antimicrobial activity is believed to be due to the ROS generation. The previous literature states the role of silver nanoparticles in generating reactive oxygen species (ROS) and eradicating bacterial populations.[30–32]

The antimicrobial activity of the SNP@PSP-incorporated creams and base cream was checked against Gram-positive organism *S. aureus* and Gram-negative organism *E. coli* and the yeast *C. albicans.* The positive controls used in the study were penicillin, gentamycin and fluconazole against *S. aureus*, *C. albicans* and *E. coli* (ESI Fig. 4†). The SNP@PSP-doped cream showed significant antimicrobial activity against *S. aureus* (Fig. 2A–C). The zone diameter increases for higher concentrations of SNP@PSP-incorporated creams. The base cream showed mild activity against *S. aureus* (Fig. 2D) but no activity against *E. coli* (Fig. 2E) and *C. albicans* (Fig. 2C). This showed that further increasing the concentrations of SNP@PSP can give rise to higher inhibition zones. Of the three formulations with different SNP@PSP concentrations, the 1% SNP@PSP cream showed the greatest anti-microbial activity. As a result, this formulation (SNP@PSP Cream 4) was chosen for

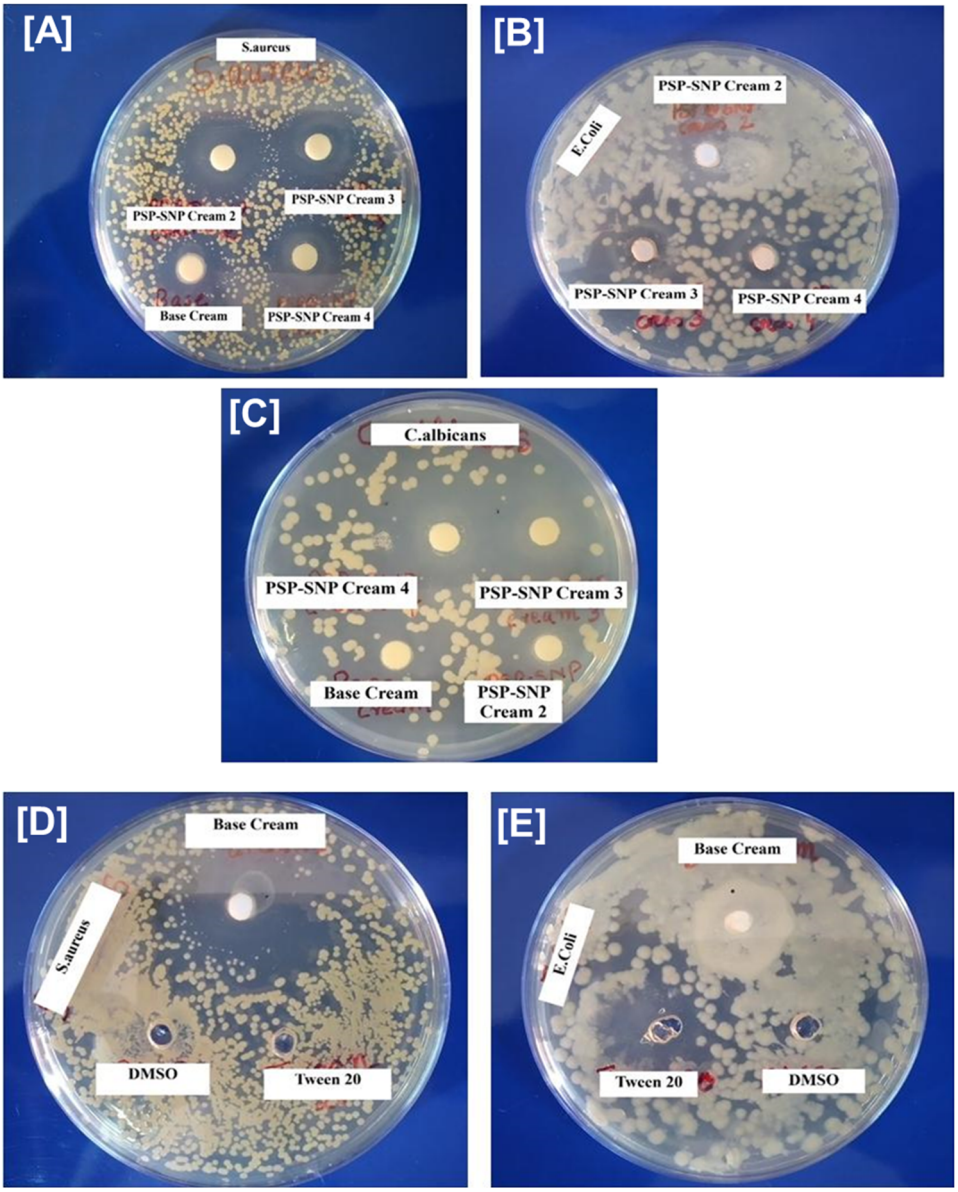

Fig. 2 Antimicrobial activity (disc diffusion method) of cream formulations on Muller Hinton agar plates toward inhibition of susceptible test organisms: (A) *S. aureus,* (B) *E. coli,* and (C) *C. Albicans*. Antimicrobial activity (well diffusion method) of Tween 20 and DMSO on Muller Hinton plates and the zone of inhibition of susceptible test organisms (D) *S. aureu* and (E) *E. coli*.

further studies. In all subsequent *in vivo* experiments, this formulation was consistently referred to as SNP@PSP cream. *S. aureus* was found to be predominant in skin infections, and hence, the results showed that in future, SNP@PSP cream formulation could be used as an effective agent against skin infections. To check whether the concentration of Tween 20 and DMSO used in the study possessed any activity, their antimicrobial activities were also studied. The results showed neither of these compounds showed any inhibition zones against *E. coli* and *S. aureus* (Fig. 2D and E).

The microbial count was determined using the total plate count (TPC) method to check the efficacy of the formulations. All the formulations were serially diluted, and each concentration was plated to check the microbial count. No growth was observed in all the concentrations of all samples (ESI Fig. 5†). This showed the effectiveness of maintaining sterile conditions during the process of cream formulation.

3.3. *In vitro* biocompatibility and wound-healing activity of SNP@PSP in human keratinocyte (HaCaT) cell lines

The MTT assay was used to analyse the cytotoxic profiling of SNP@PSP on HaCaT cell lines at different concentrations for 72 and 96 hours. The findings revealed that PSP cream and SNP@PSP were non-toxic to HaCaT cell lines, even at concentrations up to 100 μg mL^{-1} (Fig. 3A and B). At a 200 μg

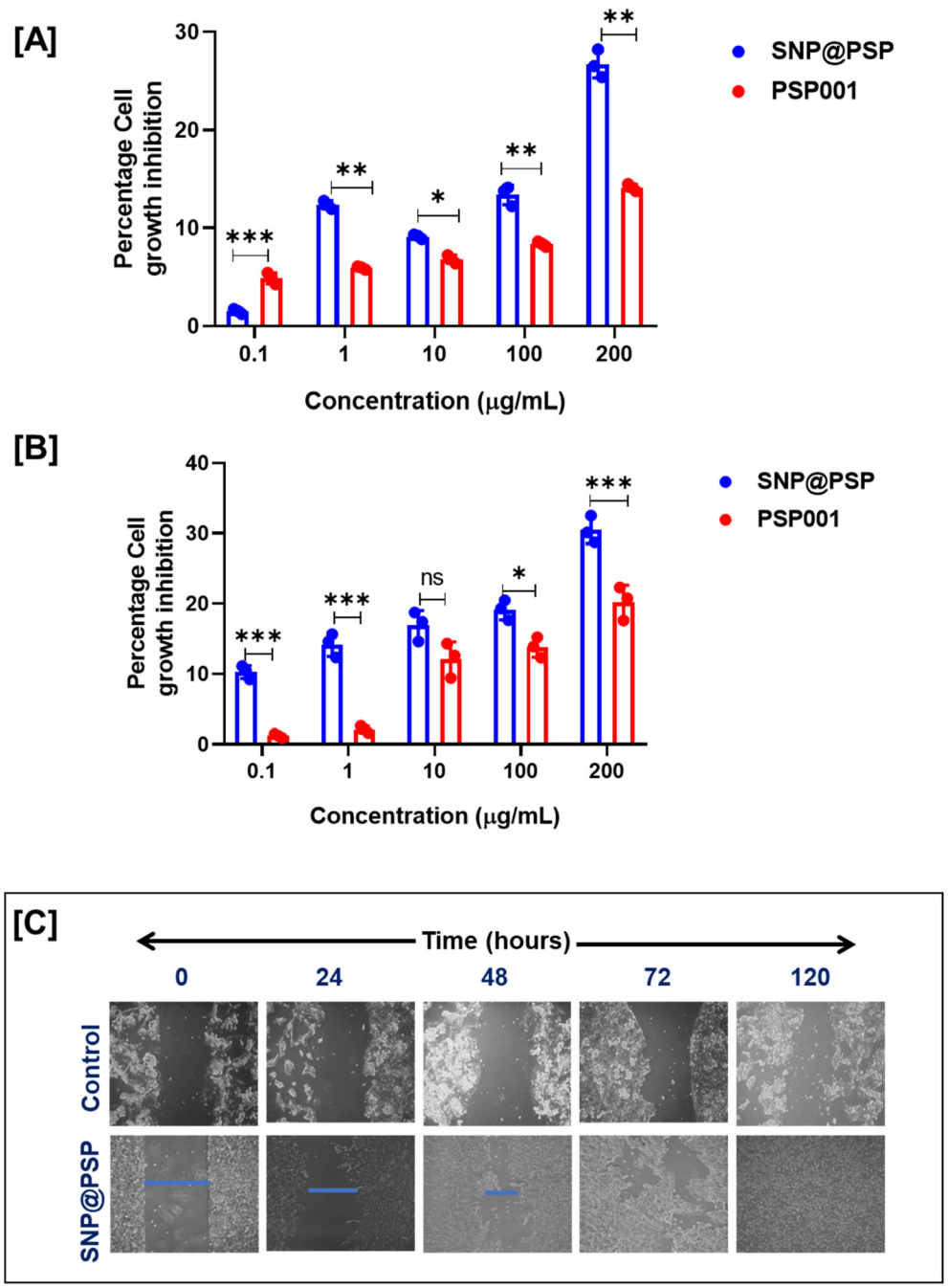

Fig. 3 Evaluation of cytotoxicity in SNP@PSP determined by MTT assay for HaCaT cell lines at (A) 72 and (B) 96 hours (n = 3). (C) *In vitro* wound-healing potential of SNP@PSP in HaCaT cell lines.

mL^{-1} concentration, cytotoxicity was less than 30%. HaCaT cells were treated with 100 μg mL^{-1} of SNP@PSP and examined under a microscope after 24 hours to observe morphological changes. Significant morphological changes leading to wound closure were detected. The results showed that SNP@PSP, at a concentration of 100 μg mL^{-1}, demonstrated significant wound-healing potential, completely closing the wounds after 120 hours, compared to the control cells (Fig. 3C and ESI Fig. 6†). The obtained area at different time points was converted to a percentage value with respect to the initial wound at zero hour, which provides the wound area using ImageJ software.[33] The wound-closure percentage was the remaining percentage of the wound area. Cultures treated with SNP@PSP exhibited faster and better cell confluency than the control. The study then focused on *in vivo* wound-healing potential, where we formulated a cream using SNP@PSP for further studies, as direct application is impossible.

3.4. *In vivo* wound-healing potential of the SNP@PSP

A cream incorporating SNP@PSP was tested using an *in vivo* wound model to determine its effectiveness. The results showed that after 14 days, the SNP@PSP-treated group exhibited significant wound healing compared to the silver-treated group (Fig. 4A). The wound reduction rate was also significantly higher in the SNP@PSP-treated group (Fig. 4B). On the 14th day, the wound treated with SNP@PSP cream 4 exhibited significant wound closure compared to the untreated group and its effect was comparable with commercially available creams. The results were compared to those of the positive control, Silverex. Our cream promoted fur regrowth more quickly than the Silverex-treated group, with no observed side effects such as irritation or itching. Swabs from the infected area showed that the SNP@PSP-incorporated cream exhibited better antimicrobial activity than the control (Fig. 5A and ESI Fig. 7†). The treated group displayed re-epithelialization of

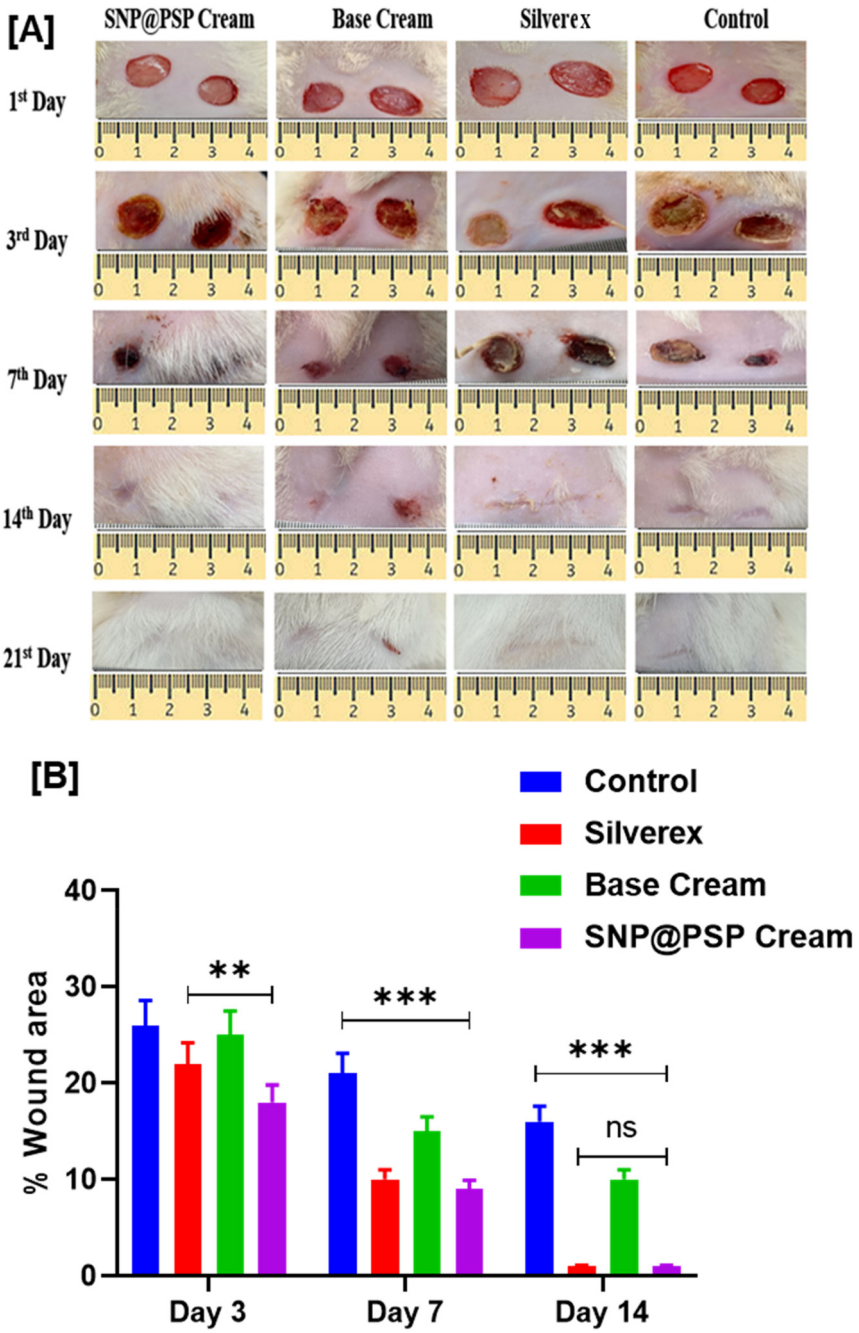

Fig. 4 (A) Dorsal excision wound of four groups of Wistar rats (control, Silverex, base cream and SNP@PSP cream) on days 1, 3, 7, 14 and 21. (B) Percentage wound area on different groups of Wistar rats on the 3rd, 7th and 14th days (n = 4).

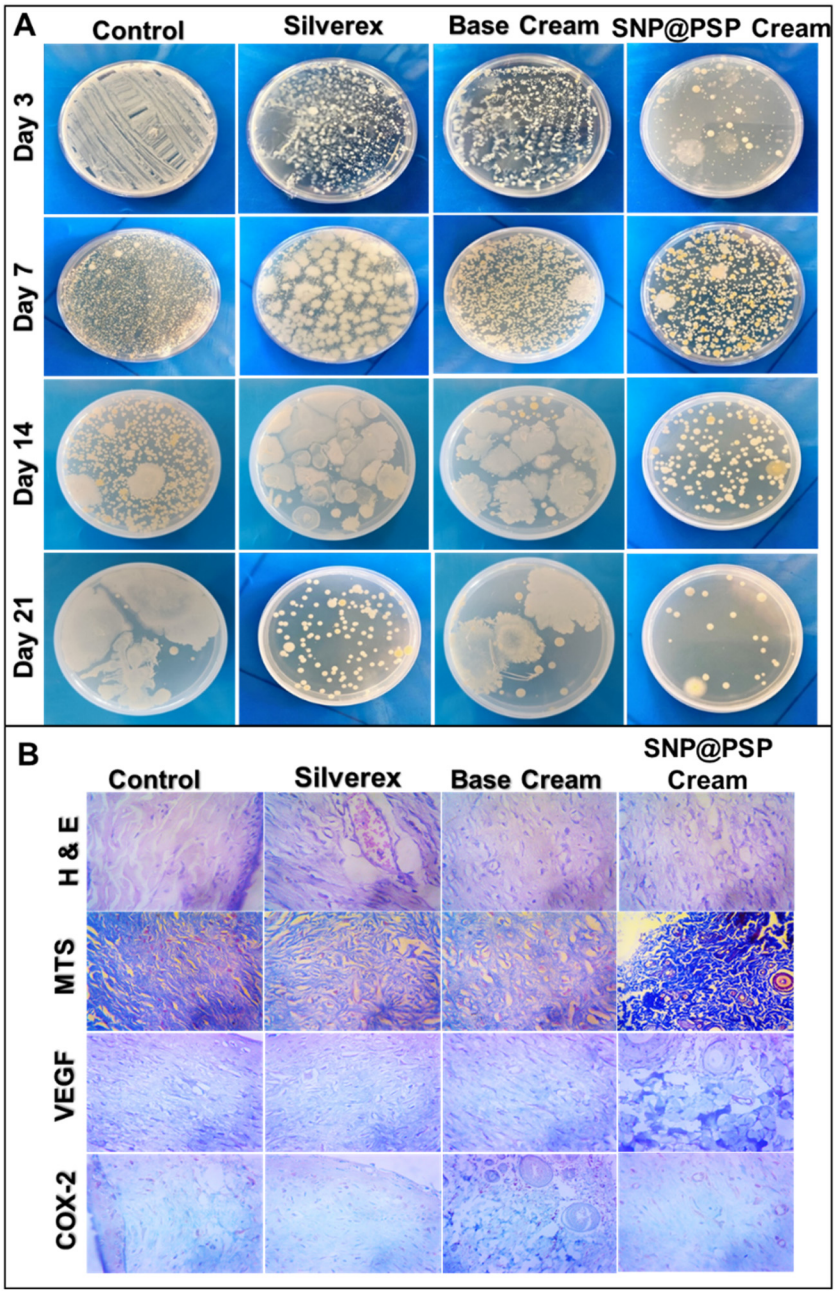

Fig. 5 (A) Microbial load around the wound area from the 1st to the 21st day. (B) H & E staining of the wound area of different treatment groups, MTS staining of wound tissue after treatment, immunohistochemistry of VEGF expression after treatment of wound tissue, and immunohistochemistry of COX 2 expression after treatment of wound tissue.

the epidermis and scattered inflammatory infiltrates, fibroblasts and thin-walled capillaries in a fibro-collagenous stroma (ESI Table 8†). COX, a housekeeping enzyme for regulating vascular homeostasis, was found to be involved in dermal homeostasis in response to injury.[27] Cox 2 and VEGF expression studies confirmed that treatment with our cream significantly reduced inflammation and resulted in faster wound healing than the control (Fig. 5B and ESI Table 9†). The expression of COX-2 serves as an indicator of acute inflammation, graded on a scale from negative (0) to 3+, representing the immunoreactive levels of COX-2. In our study, the semi-quantitative assessment of COX-2 levels showed significantly lower expression in the SNP@PSP cream-treated group compared to the control, indicating the absence of active inflammation in the wound area. Additionally, VEGF levels were also negative, confirming the lack of early granulation tissue formation. Microscopic examination and MTS staining revealed that the SNP@PSP cream-treated group exhibited normal tissue architecture, whereas the Silverex-treated group showed evidence of collagen

accumulation and fibrotic regions, indicative of early scar formation. These findings suggest that our SNP@PSP-loaded cream demonstrates a better therapeutic response when compared to the positive control, namely Silverex, by promoting wound healing without excessive scarring.[34]

4. Conclusion

The current investigation successfully formulated a biocompatible cream for wound-healing applications using naturally derived, under-utilized polysaccharide PSP001 isolated from *Punica grantum*. To enhance the antimicrobial property of the cream formulation, we synthesised silver nanoparticles using this PSP001 and doped it into the cream. No change was observed in the organoleptic and physiochemical properties of the cream. The formulation was also found to be stable under all extreme conditions. The cream was found to be compatible with BIS specifications. The results showed that these formulations were effective against *S. aureus* and *C. albicans*, key organisms for a prolonged wound-healing process. *In vivo*, the wound-healing potential of all formulations was significantly comparable with the positive control, Silverex cream. Moreover, thorough toxicological analyses using Masson trichome-stained wound sections and histology helped rule out potential off-target effects. The ability of the cream to treat wounds was also proven by immunohistochemistry analysis. Therefore, the antibacterial properties, cost-effectiveness, biocompatibility, and wound-healing ability of this specially formulated cream were real and highly significant advantages. The findings of this study can open the door to creating an affordable biocompatible scaffold with antibacterial and wound-healing properties from leftover biowaste. This work has been awarded an Indian patent (Patent No. 464226) on 31/10/2023.

Data availability

The data supporting this article have been included as part of the ESI.†

Conflicts of interest

The authors declare there is no conflict of interest.

Acknowledgements

The authors would like to thank the Department of Health Research, the Indian Council of Medical Research, and the Government of India for financially supporting this study through the Young Scientist Fellowship (YSS/2019/000015/PRCYSS).

References

1 G. K. Srivastava, S. Martinez-Rodriguez, N. I. Md Fadilah, D. Looi Qi Hao, G. Markey, P. Shukla, *et al.*, Progress in wound-healing products based on natural compounds, stem cells, and microRNA-based biopolymers in the European, USA, and Asian markets: Opportunities, barriers, and regulatory issues, *Polymers*, 2024, **16**(9), 1280.
2 M. B. Dreifke, A. A. Jayasuriya and A. C. Jayasuriya, Current wound healing procedures and potential care, *Mater. Sci. Eng., C*, 2015, **48**, 651–662.
3 M. Gupta, U. Agrawal and S. P. Vyas, Nanocarrier-based topical drug delivery for the treatment of skin diseases, *Expert Opin. Drug Delivery*, 2012, **9**(7), 783–804.
4 A. Weintraub, Immunology of bacterial polysaccharide antigens, *Carbohydr. Res.*, 2003, **338**(23), 2539–2547.
5 B. Unnikrishnan, A. Sen, G. Preethi, M. M. Joseph, S. Maya, R. Shiji, *et al.*, Folic acid-appended galactoxyloglucan-capped iron oxide nanoparticles as a biocompatible nanotheranostic agent for tumor-targeted delivery of doxorubicin, *Int. J. Biol. Macromol.*, 2021, **168**, 130–142.
6 B. Unnikrishnan, S. Maya, G. Preethi, K. Anusree, P. Reshma, M. Archana, *et al.*, Self-assembled drug loaded glycosyl-protein metal nanoconstruct: detailed synthetic procedure and therapeutic effect in solid tumor treatment, *Colloids Surf., B*, 2020, **193**, 111082.
7 B. Unnikrishnan, G. Preethi, S. Anitha, R. Shiji, M. Archana, J. Sreekutty, *et al.*, Impact of Galactoxyloglucan Coated Iron Oxide Nanoparticles on Reactive Oxygen Species Generation and Magnetic Resonance Imaging for Tumor Management, *J. Cluster Sci.*, 2022, 1–14.
8 M. M. Joseph, S. Aravind, S. Varghese, S. Mini and T. Sreelekha, Evaluation of antioxidant, antitumor and immunomodulatory properties of polysaccharide isolated from fruit rind of Punica granatum, *Mol. Med. Rep.*, 2012, **5**(2), 489–496.
9 P. B. Albuquerque, P. A. Soares, A. C. Aragão-Neto, G. S. Albuquerque, L. C. Silva, M. H. Lima-Ribeiro, *et al.*, Healing activity evaluation of the galactomannan film obtained from Cassia grandis seeds with immobilized Cratylia mollis seed lectin, *Int. J. Biol. Macromol.*, 2017, **102**, 749–757.
10 L. Fan, Y. Du, B. Zhang, J. Yang, J. Zhou and J. F. Kennedy, Preparation and properties of alginate/carboxymethyl chitosan blend fibers, *Carbohydr. Polym.*, 2006, **65**(4), 447–452.
11 N. I. M. Fadilah, S. J. Phang, N. Kamaruzaman, A. Salleh, M. Zawani, A. Sanyal, *et al.*, Antioxidant biomaterials in cutaneous wound healing and tissue regeneration: A critical review, *Antioxidants*, 2023, **12**(4), 787.
12 R. Ghosh Auddy, M. F. Abdullah, S. Das, P. Roy, S. Datta and A. Mukherjee, New guar biopolymer silver nanocomposites for wound healing applications, *BioMed Res. Int.*, 2013, **2013**(1), 912458.
13 M. G. Miguel, M. A. Neves and M. D. Antunes, Pomegranate (Punica granatum L.): A medicinal plant with

myriad biological properties-A short review, *J. Med. Plants Res.*, 2010, **4**(25), 2836–2847.
14 K. Ayswarya, *Phytochemical screening and antioxidant evaluation of Pomegranate (Punica granatum L.) WINE*. 2022.
15 D. Prashanth, M. Asha and A. Amit, Antibacterial activity of Punica granatum, *Fitoterapia*, 2001, **72**(2), 171–173.
16 S. Ghosh, A. Samanta, N. B. Mandal, S. Bannerjee and D. Chattopadhyay, Evaluation of the wound healing activity of methanol extract of Pedilanthus tithymaloides (L.) Poit leaf and its isolated active constituents in topical formulation, *J. Ethnopharmacol.*, 2012, **142**(3), 714–722.
17 M. M. Joseph, J. B. Nair, K. K. Maiti and T. S. Therakathinal, Plasmonically enhanced galactoxyloglucan endowed gold nanoparticles exposed tumor targeting biodistribution envisaged in a surface-enhanced Raman scattering platform, *Biomacromolecules*, 2017, **18**(12), 4041–4053.
18 M. M. Joseph, J. B. Nair, R. N. Adukkadan, N. Hari, R. K. Pillai, A. J. Nair, *et al.*, Exploration of biogenic nanochemobiotics fabricated by silver nanoparticle and galactoxyloglucan with an efficient biodistribution in solid tumor investigated by SERS fingerprinting, *ACS Appl. Mater. Interfaces*, 2017, **9**(23), 19578–19590.
19 C. Kong, S. Chen, W. Ge, Y. Zhao, X. Xu, S. Wang, *et al.*, Riclin-capped silver nanoparticles as an antibacterial and anti-inflammatory wound dressing, *Int. J. Nanomed.*, 2022, 2629–2641.
20 H. Syama, B. Unnikrishnan, J. Sreekutty, M. Archana, M. M. Joseph, G. Preethi, *et al.*, Bio fabrication of galactomannan capped silver nanoparticles to apprehend Ehrlich ascites carcinoma solid tumor in mice, *J. Drug Delivery Sci. Technol.*, 2022, **76**, 103649.
21 H. Padinjarathil, M. M. Joseph, B. Unnikrishnan, G. Preethi, R. Shiji, M. Archana, *et al.*, Galactomannan endowed biogenic silver nanoparticles exposed enhanced cancer cytotoxicity with excellent biocompatibility, *Int. J. Biol. Macromol.*, 2018, **118**, 1174–1182.
22 C. Ferrero and M. Jiménez-Colomina, Rheological behavior of creams and semi-solid systems, *J. Cosmet. Sci.*, 2014, **65**(5), 325–340.
23 R. Lapasin and S. Pricl, *Rheology of industrial polysaccharides: theory and applications*, Springer Netherlands, 1995.
24 A. Ahuja, R. K. Khar and J. Ali, Rheological study of topical gels: a review, *Drug Dev. Ind. Pharm.*, 2005, **31**(7), 615–620.
25 R. H. Müller and C. Jacobs, Nanosuspensions as particulate drug formulations in therapy: rationale for development and what we can expect for the future, *Adv. Drug Delivery Rev.*, 2002, **54**(1), 131–155.
26 F. Cappiello, B. Casciaro and M. L. Mangoni, A novel in vitro wound healing assay to evaluate cell migration, *J. Visualized Exp.*, 2018, **133**, e56825.
27 S. A. Pileri, G. Roncador, C. Ceccarelli, M. Piccioli, A. Briskomatis, E. Sabattini, *et al.*, Antigen retrieval techniques in immunohistochemistry: comparison of different methods, *J. Pathol.*, 1997, **183**(1), 116–123.
28 M. M. Joseph, S. Aravind, S. K. George, S. Varghese and T. Sreelekha, A galactomannan polysaccharide from Punica granatum imparts in vitro and in vivo anticancer activity, *Carbohydr. Polym.*, 2013, **98**(2), 1466–1475.
29 C. Wang, X. Gao, Z. Chen, Y. Chen and H. Chen, Preparation, characterization and application of polysaccharide-based metallic nanoparticles: a review, *Polymers*, 2017, **9**(12), 689.
30 H. Xu, F. Qu, H. Xu, W. Lai, Y. Andrew Wang, Z. P. Aguilar, *et al.*, Role of reactive oxygen species in the antibacterial mechanism of silver nanoparticles on Escherichia coli O157: H7, *BioMetals*, 2012, **25**, 45–53.
31 B. Das, S. K. Dash, D. Mandal, T. Ghosh, S. Chattopadhyay, S. Tripathy, *et al.*, Green synthesized silver nanoparticles destroy multidrug resistant bacteria via reactive oxygen species mediated membrane damage, *Arabian J. Chem.*, 2017, **10**(6), 862–876.
32 M. Huang, K. Ye, T. Hu, K. Liu, M. You, L. Wang, *et al.*, Silver nanoparticles attenuate the antimicrobial activity of the innate immune system by inhibiting neutrophil-mediated phagocytosis and reactive oxygen species production, *Int. J. Nanomed.*, 2021, 1345–1360.
33 A. Suarez-Arnedo, F. T. Figueroa, C. Clavijo, P. Arbeláez, J. C. Cruz and C. Muñoz-Camargo, An image J plugin for the high throughput image analysis of in vitro scratch wound healing assays, *PLoS One*, 2020, **15**(7), e0232565.
34 R. Singh and J. E. Brinchmann, Nanomedicine: advancements in wound healing using nanotechnology-based approaches, *Front. Physiol.*, 2018, **9**, 913.